Mechanism of Copper Mediated Triple Helix Formation at Neutral pH in *Drosophila* Satellite Repeats

C. Paris,*† F. Geinguenaud,*† C. Gouyette,‡ J. Liquier,*† and J. Lacoste*†

*Laboratoire de Biophysique Moléculaire, Cellulaire et Tissulaire (BioMoCeTi), Unité Mixte de Recherche, Centre National de la Recherche Scientifique 7033, Unité de Formation et de Recherche, Santé, Médecine et Biologie Humaine, Université Paris 13, 93017 Bobigny cedex, France; †Université Pierre et Marie Curie, Case 138, 75252 Paris cedex 05, France; and ‡Plate-forme Synthèse d'Oligonucléotides, Institut Pasteur, 75724 Paris cedex 15, France

ABSTRACT The highly repeated *Drosophila melanogaster* AAGAGAG satellite sequence is present at each chromosome centromere of the fly. We demonstrate here how, under nearly physiological pH conditions, these sequences can form a pyrimidine triple helix containing T·A-T and C^{Cu}·G-C base triplets, stabilized by Cu^{2+} metal ions in amounts mirroring in vivo concentrations. Ultraviolet experiments were used to monitor the triple helix formation at pH 7.2 in presence of Cu^{2+} ions. Triplex melting is observed at 23°C. Furthermore, a characteristic signature of triple helix formation was obtained by Fourier transform infrared spectroscopy. The stabilization of the C·G-C base triplets at pH 7.2 is shown to occur via interactions of Cu^{2+} ions on the third strand cytosine N3 atom and on the guanine N7 atom of the polypurine target strand forming C^{Cu}·G-C triplets. Under the same neutral pH conditions in absence of Cu^{2+} ions, the triple helix fails to form. Possible biological implications are discussed.

INTRODUCTION

Various divalent metal ions are known to interact with nucleic acids both in vitro and in vivo (1). Most investigations underlined the important role of metal ions in various functions of DNA in vivo. For example these metal ions can influence the synthesis rate and the accuracy of the nucleotide sequence in DNA—and RNA—polymerase systems (2), participate in the formation of protein nucleic acid complexes (3), promote non-B DNA structures (4,5), or even cause mutagenesis and carcinogenesis (2,6).

It has been well known for a long time that, in vivo, traces of divalent metal ions are preferentially bound to reiterative DNA sequences (7) and since such DNA sequences are essentially present in constitutive heterochromatin areas it was interesting to consider more precisely the properties of these sequences and their function, taking into account the presence of metal ions at some steps of the mitotic cycle.

Constitutive heterochromatin areas occupy identical positions in homologous chromosomes and were first distinguished from euchromatin areas on the basis of differential staining with banding techniques (8). Heterochromatin is especially abundant at the centromeres and telomeres. It is composed of highly reiterated sequences called satellite DNA, characterized by their unusual base composition and nature. For example, in *Drosophila melanogaster*, heterochromatin accounts for an estimated 33.5% of the female genome with satellite repeats representing 21% of the genome (9,10). Progress has been made in the understanding of the sequence and molecular organization of *Drosophila* (9,11,12) and human (13) centromeres, yet our understanding of their higher structural organization and function is still very limited. Molecular and genetic properties that further distinguish heterochromatin from euchromatin include condensation throughout the cell cycle, late replicating during S phase, and faster replicating DNA leading to a good synchrony of its replication, transcriptional inactivity, sequence composition, and greater contents of metal ions (6).

Among these metal ions, copper seems to play an important role in heterochromatin structure and function (2,6). The binding of Cu^{2+} to DNA appears to be highly cooperative and related to DNA denaturation. Moreover the Cu^{2+} binding is concentration dependent. At very low metal concentration Cu^{2+} binds nonspecifically to the phosphate groups like most other ions. Upon increasing concentration, the Cu^{2+} ions begin to reach the bases mostly by chelation with the N7 of guanine. When metal ion concentration reaches 0.7 atom/nucleotide, the double helix is opened, and DNA denaturation begins (2,6,14,15). Several models have been proposed to describe the Cu^{2+} binding to double-stranded DNA that we will not discuss here (7,16). Considering these properties, it is clear that Cu^{2+} binding to DNA can influence the structures and the functions of heterochromatic areas in vivo in various ways. For example Cu^{2+} can cause DNA helix-coil transition—thus facilitating replication, inducing errors during translation—or even be implicated in carcinogenesis (6,7). On the other hand, copper is known to be able, like other divalent cations, to promote and stabilize non-B DNA structures (5,16–18) and even triple helices (19).

A DNA triplex is formed upon binding of a pyrimidine or a purine single-stranded DNA to the major groove of a double helix, forming Hoogsteen or reverse-Hoogsteen hydrogen bonds with the purine strand of the duplex. Triplex DNA comes in three structural classes that differ in the base composition of the third strand, the relative orientation of the phosphodiester backbones, the sensitivity to pH and cations

Submitted October 23, 2006, and accepted for publication December 8, 2006.

Address reprint requests to J. Lacoste, Tel.: 33-1-48-38-73-91; Fax: 33-1-48-38-73-56; E-mail: jerl@ccr.jussieu.fr.

0006-3495/07/04/2498/09 $2.00

doi: 10.1529/biophysj.106.099788

(4,17), and thermodynamic parameters (20). They have been described as the (C, T) or pyrimidine motif, the (G, A) or purine motif, and the (G, T) motif. These motifs can form both intramolecularly, giving H DNA, and intermolecularly with triple helix-forming oligonucleotides (TFOs). In the pyrimidine motif, the third strand is composed of cytosines and thymines and binds parallel to the purine strand of the duplex by Hoogsteen hydrogen bonds, leading to the formation of T·A-T and C^+·G-C triplets (21,22). (In the triple helix notation, the (·) represents the hydrogen bonds between the third strand and the target duplex; the (-) represents the Watson-Crick hydrogen bonds.) Formation of this motif requires slightly acidic conditions (21,22). In the purine motif, the third strand is composed of guanines and adenines and binds antiparallel to the purine strand of the duplex by reverse-Hoogsteen hydrogen bonds, leading to the formation of A·A-T and G·G-C triplets (21–23). This motif contains no protonated bases and its stability is therefore pH independent; however its formation generally requires divalent (Mg^{2+}, Zn^{2+}, Mn^{2+}, etc.) (17) or multivalent cations (spermine, spermidine) (22). In the (G, T) motif the third strand is composed of guanines and thymines and binds parallel or antiparallel to the purine strand of the duplex, depending on the number of TpG steps in the third strand (24–26).

We have recently shown using electrophoretic mobility shift assay experiments that low concentrations of Cu^{2+} can promote the formation and stabilization of a pyrimidine triplex with *D. melanogaster* satellite repeats under nearly physiological condition (i.e., mostly neutral pH), bypassing the protonation requisite of the third strand cytosines (19).

Fourier transform infrared (FTIR) spectroscopy has been widely used for investigating metals in interaction with DNA (15,27,28) and is known to be an appropriate technique to evidence the formation of triple helical structures and to determine many of their characteristics (basepairing, sugar geometries, etc.) (29,30). In this work we investigate by FTIR and ultraviolet (UV) spectroscopies the in vitro formation of a pyrimidine triplex at neutral pH in presence of Cu^{2+} by the *D. melanogaster* satellite sequence $(AAGAGAG)_{n=2}$. We then propose a mechanism by which the Cu^{2+} ions can overcome the protonation requisite for classical pyrimidine motif triple helices and promote the triple helix formation at neutral pH.

MATERIALS AND METHODS

Oligonucleotides

The oligonucleotides were synthesized on an automatic Applied Biosystems 3400 synthesizer (Applied Biosystems, Foster City, CA) using controlled pore glass beads support and the phosphoramidite chemistry. After synthesis the oligonucleotides were cleaved from the support by concentrated ammonia at room temperature and then deprotected overnight at 55°C always in ammonia.

After evaporation to dryness, the oligonucleotides were desalted on a G10 Sephadex column and then purified twice by high-performance liquid chromatography (HPLC) on a reverse phase C18 column using gradient CH_3CN in TEAAc buffer. The purified oligonucleotides were then exchanged into sodium salt on a Dowex Na^+ column and lyophilized. Purity was checked by analytical HPLC, capillar electrophoresis, and matrix-assisted laser desorption ionization-time of flight. For vibrational spectroscopy three 14-mer deoxyoligonucleotides were synthesized with the following sequences:

purine strand of the duplex: 5′ AAGAGAGAAGAGAG 3′ called 14R;
pyrimidine strand of the duplex: 5′ CTCTCTTCTCTCTT 3′ called 14Y;
third strand (TFO): 5′ TTCTCTCTTCTCTC 3′ called 14TC;
selective deuteration of the guanines in the 14R strand was obtained by dissolving the oligonucleotide in D_2O and heating for 1 h at 85°C (31);
for UV measurements an extended target duplex formed by two 26-mers incorporating the 14R and 14Y sequences was used;
purine strand of the duplex: 5′ CTTGCC AAGAGAGAAGAGAG CATGTC 3′ called 26R;
pyrimidine strand of the duplex: 5′ GACATG CTCTCTTCTCTCTT GGCAAG 3′ called 26Y.

Concentrations of oligonucleotides were estimated by UV absorption measurements at 85°C using a nearest-neighbor approximation for the absorption coefficients (32). All concentrations are expressed in strand molarities.

UV spectroscopy

Absorbance versus temperature cooling and heating curves were obtained using a UVIKON 940 (Kontron, Paris, France) spectrophotometer as previously described (19). The temperature of the bath was increased or decreased at a rate of 0.1°C/min, thus allowing complete thermal equilibrium of the cells. At each temperature, absorbance measurements were performed at 245, 260, and 330 nm (control wavelength). Data were extracted from the profiles recorded at 260 nm. Unless otherwise specified, all experiments were performed in 10 mM sodium cacodylate buffer (pH 6.0 or 7.2) containing 25 mM KCl and between 0 and 35 μM $CuCl_2$ (0–0.5 copper ions/nucleotide). For triplex experiments strand concentrations were 1 μM for the duplex and 1.2 μM for the third strand. T_m was determined as described in Rougée et al. (33). In all UV experiments, the extended target duplex was used shifting, as previously described (19), the duplex melting toward higher temperatures to distinguish triplex from duplex transition.

Infrared spectroscopy

The 14RY duplexes were preformed and annealed at 95°C for 10 min. The desired amount of Cu^{2+} ions ($CuCl_2$ solution) was then added. Finally an equimolecular amount of third strand (in the same buffer as the duplex) was added.

Samples were studied in H_2O and in D_2O solutions at a strand concentration around 10 μM. They were deposited between two ZnSe windows without spacer. Deuteration experiments were performed by drying the samples under nitrogen and redissolving them in identical volumes of D_2O (>99.8% purity, Euriso-Top; CEA, Saclay, France). FTIR spectra were recorded using a Perkin Elmer 2000 spectrophotometer (Perkin Elmer, Foster City, CA) at a 1-cm^{-1} resolution. Five scans were accumulated. Data treatment was performed using the Perkin Elmer spectrum program.

RESULTS AND DISCUSSION

UV melting curve analysis

Formation of pyrimidine triple helices can be monitored by following the UV absorbance. We first performed melting experiments with the same 14-basepair duplex (14RY) as

TABLE 1 T_m values from UV experiments

	T_m (°C)						
	pH 6.0 25 mM KCl 0 Cu^{2+}/Po	pH 6.0 50 mM KCl 0 Cu^{2+}/Po	pH 6.0 140 mM KCl 0 Cu^{2+}/Po	pH 7.2 25 mM KCl 0 Cu^{2+}/Po	pH 7.2 25 mM KCl 0.15 Cu^{2+}/Po*	pH7.2 25 mM KCl 0.33 Cu^{2+}/Po†	pH 7.2 25 mM KCl 0.5 Cu^{2+}/Po‡
Triplex	36	36	36	–	–	–	23
Duplex	57	62	67	57	57	57	57

When hysteresis is present, T_m values provided here correspond to the heating curve. All T_m values determined at 260 nm are given with an incertitude of ±1°C. A dash means no transition. All experiments are performed in 10 mM sodium cacodylate pH 6.0 or pH 7.2 in 25–140 mM KCl with *10.5 μM $CuCl_2$ (0.15 copper ion/nucleotide), †23 μM $CuCl_2$ (0.33 copper ion/nucleotide), or ‡35 μM $CuCl_2$ (0.5 copper ion/nucleotide).

used in infrared experiments. Under these conditions triplex and duplex melting transitions appeared to be intermingled, prohibiting an accurate T_m determination. We thus chose to use a 26-basepair duplex to shift the duplex transition to higher temperatures. All T_m values are reported in Table 1, and melting curves for some conditions are illustrated in Fig. 1.

Curves *a* and *b* are controls showing the behavior with increasing temperature of the third 14TC TFO strand alone at pH 6 (*curve a*) and at pH 7.2 in presence of 0.5 Cu^{2+} ion/nucleotide (*curve b*). In both cases no transition is detected, showing that no third strand association occurs under the conditions used to prepare the triplexes.

At pH 6.0 in 25 mM KCl, for the equimolecular mixture of the 26RY duplex and the 14TC third strand a classical pyrimidine triple helix melting curve is obtained (Fig. 1, *curve e*). A first clear transition due to the separation of the TFO from the duplex is detected with a T_m value of 36°C, whereas the duplex transition exhibits a T_m value of 57°C (Table 1, column 1) at the same temperature as that measured for the duplex alone under similar conditions (Fig. 1, *curve c*). As expected, an increase in KCl ionic strength induces a stabilization of the duplex to 67°C (Table 1, columns 2 and 3), whereas the triplex T_m remains unchanged, as previously described in Horn et al. (19).

At pH 7.2 in 25 mM KCl when the 26RY duplex is mixed with the 14TC TFO, no transition due to the formation of a triple helix can be evidenced (Table 1, column 4). Under the same conditions and in presence of Cu^{2+} ions with a ratio of 0.15 and 0.33 Cu^{2+}/nucleotide, still only monophasic melting curves are obtained, corresponding to the 26RY duplex transition (Table 1, columns 5 and 6, curves not shown). At a ratio of 0.5 Cu^{2+} ions/nucleotides a biphasic melting curve is recorded (Fig. 1, *curve f*). The first transition with a T_m value of 23°C can be assigned to the separation of the third strand from the duplex, whereas the second transition observed at 57°C corresponds to the melting of the 26RY duplex (Table 1, column 7). This latter transition is observed at the same temperature as for the 26RY duplex alone in presence of copper ions (Fig. 1, *curve d*). It should be noted that for curve 1 *d*, upon cooling, around 40°C a slight displacement of the curve is observed, reflecting the difficulty in reforming the duplex in presence of Cu^{2+} ions. A similar displacement, upon cooling, is observed for curve 1 *f* above the triplex T_m.

In presence of copper the triplex transition at 23°C appears perfectly reversible upon association (cooling) and dissociation (heating) (Fig. 1, *curve f*) in contrast with classical pyrimidine triplexes for which, at acidic pH, the dissociation is generally shifted toward higher temperatures as compared to the association curves (Fig. 1, *curve e*, and (19,33)). This reflects that the mechanism by which the triplex formation is

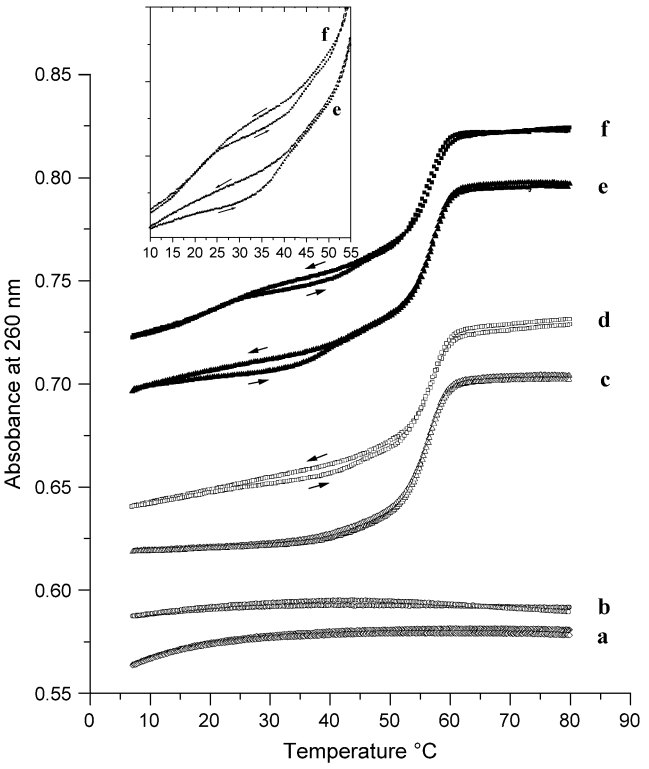

FIGURE 1 UV melting curves. All experiments are performed in 10 mM sodium cacodylate pH 6.0 or pH 7.2 and 25 mM KCl unless otherwise specified. Strand concentrations are for triplex experiments: 1 μM for the duplex and 1.2 μM for the third strand; for duplex experiments 1 μM for each strand of the duplex; and for control experiments: 2.5 μM of 14TC TFO. (*a*) Self-association of the 14TC TFO at acidic pH. (*b*) Self-association of the 14TC TFO at neutral pH in presence of $CuCl_2$ (0.5 copper ion/nucleotide). (*c*) 26RY duplex formation at acidic pH. (*d*) 26RY duplex formation at neutral pH in presence of $CuCl_2$ (0.5 copper ions/nucleotide). (*e*) Triple helix formation at acidic pH. (*f*) Triple helix formation at neutral pH in presence of $CuCl_2$ (0.5 copper ion/nucleotide). (*Inset*) expanded absorbance scale evidencing the triplex melting in curves *e* and *f*.

achieved in presence of copper ions is clearly different from that occurring under acidic pH conditions.

Thus UV experiments show that Cu^{2+} ions are able to stabilize a triple helix formed by the $(AAGAGAG)_{n=2}$ *Drosophila* satellite repeats at neutral pH. To further investigate the mechanism of this stabilization, we have studied this triple helix by vibrational spectroscopy, which allows us to probe different putative interaction sites in nucleic acid structures.

Vibrational spectroscopy

Binding of copper ions on the 14TC oligonucleotide

Fig. 2 presents the FTIR spectra of the 14TC oligonucleotide in absence (spectrum 2 *a*) and in presence of increasing amounts of Cu^{2+} ions (0.5 Cu^{2+}/nucleotide, spectrum 2 *b*; 1 Cu^{2+}/nucleotide, spectrum 2 *c*). The spectra are recorded in D_2O solutions, and the spectral domain shown (1750–1450 cm^{-1}) contains absorption bands due to in-plane double bond stretching vibrations of the bases. The base absorption bands of the 14TC spectrum can be assigned as follows (Table 2 column 3): 1693 cm^{-1} thymine C2=O2 stretching vibration; 1660 cm^{-1}, thymine C4=O4 stretching vibration (band overlapping the 1653 cm^{-1} cytosine C2=O2 stretching vibration absorption); 1634 cm^{-1}: thymine ring vibration; 1524 and 1506 cm^{-1}: cytosine ring vibrations (30,34). The 1524 cm^{-1} band involves in particular the motions of the cytosine N3 atom (35). Progressive addition of Cu^{2+} ions shifts this band to higher wavenumbers (1546 cm^{-1}), reflecting the interaction of the copper ions on the N3 cytosine site. A similar shift of the 1524 cm^{-1} band to 1546 cm^{-1} is also observed upon addition of Cu^{2+} to dC_{14} or poly dC (spectra not shown). The 1506 cm^{-1} cytosine ring vibration is also affected by the addition of copper ions. It progressively disappears with increasing copper content and is replaced by an absorption located at 1518 cm^{-1}. Binding of copper on the cytosine affects the electronic repartition of the ring and thus possibly the relative intensity of the 1506 cm^{-1} band. Earlier NMR (36) and infrared (IR) (16,37) studies have shown that Cu^{2+} does not bind to thymidine. We notice that the addition of Cu^{2+} ions to the 14TC oligonucleotide does not alter the positions of the three thymine bands described above. In summary, the Cu^{2+} ions interact with the cytosines of the free 14TC third strand at the position of the N3 atoms.

Effect of copper ions on the targeted duplex

Fig. 2, *d–f*, presents the FTIR spectra of the 14RY duplex under the same ionic conditions as discussed above for the single-strand 14TC. In absence of copper the duplex spectrum bands (Fig. 2 *d*) can be assigned as follows (Table 2, column 6): 1696 cm^{-1} thymine C2=O2 stretching; 1674 cm^{-1} guanine C6=O6 stretching; 1656 cm^{-1} overlap of thymine C4=O4 and cytosine C2=O2 stretching; 1637 cm^{-1}: thymine ring vibration; 1623 cm^{-1} adenine ND_2 bending coupled to a ring vibration; 1577 and 1564 cm^{-1}: guanine ring vibrations; 1501 cm^{-1} cytosine ring vibration. We observe here that the absorption of cytosine at 1524 cm^{-1} detected in the case of a free cytosine is no longer present; this shows the involvement of the N3 site in the Watson-Crick G-C basepair. Addition of Cu^{2+} ions in a ratio of 0.5 Cu^{2+}/nucleotide does not alter the FTIR spectrum of the duplex (Fig. 2 *e*). If the metal content is increased to 1 Cu^{2+} ion/nucleotide, important modifications of the spectrum are detected (Fig. 2 *f*). These changes, described below, are in agreement with the previously observed effect of the addition of copper to native calf thymus DNA, which was interpreted as reflecting a conformational transition from a B geometry to some intermediate conformation that is

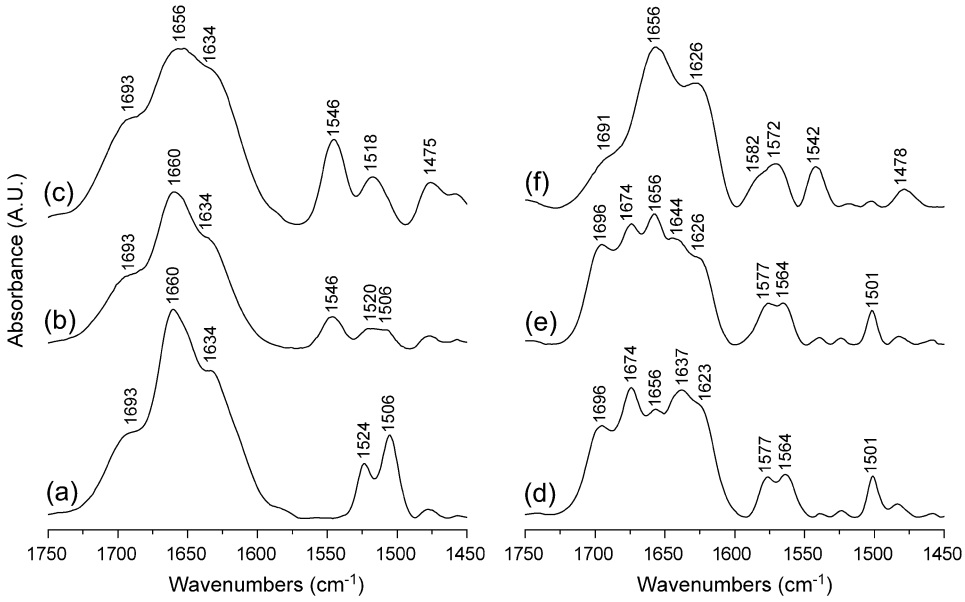

FIGURE 2 FTIR spectra recorded in D_2O solutions at pH 7.2 in the base in-plane double bond stretching vibration range (1750–1450 cm^{-1}) of (*a*) single 14TC strand; (*b*) single 14TC strand with 0.5 Cu^{2+} ion/nucleotide; (*c*) single 14TC strand with 1 Cu^{2+} ion/nucleotide; (*d*) duplex 14RY; (*e*) duplex 14RY with 0.5 Cu^{2+} ion/nucleotide; and (*f*) duplex 14RY with 1 Cu^{2+} ion/nucleotide.

TABLE 2 Proposed assignments of base in-plane stretching vibration bands observed in D_2O solutions of the single strands duplexes and triple helices

dC_{14}*	dT_{12} (43)	14TC and 14Y		14R*	14RY			14RY + 14TC			
pH7	pH7	pH7		pH7	pH7			pH7		pH6	
		0 Cu^{2+}	1 Cu^{2+}	0 Cu^{2+}	0 Cu^{2+}	0.5 Cu^{2+}	1 Cu^{2+}	0 Cu^{2+}	0.5 Cu^{2+}	0 Cu^{2+}	Assignment
									1702	1702	
	1695	1693	1693		1696	1696	1691	1696			C2=O2 T
				1670	1674	1674		1674			C6=O6 G
1653	1663	1660	1656		1656	1656	1656	1656	1656	1656	C2=O2 C
											C4=O4 T
	1632	1634	1634		1637	1644		1637	1632		Ring T
				1626	1623	1626	1626	1623			δND_2+ring A
1619											Ring C
							1582		1582		Ring G
				1579	1577	1577	1572	1577	1572	1577	Ring G
				1564	1564	1564		1564	1564	1564	Ring G
			1546				1542		1540		Ring C-Cu^{2+}
1524		1524						1520			Ring C
			1518								Ring C-Cu^{2+}
1506		1506			1501	1501		1501	1501	1501	Ring C

*Spectra not shown.

inconsistent with either the A- or Z-form or a completely denatured state (38). In fact we observe the decrease of the 1501 cm^{-1} band, the emergence of a 1478 cm^{-1} band, and the presence of a band at 1582 cm^{-1} (this last band reflects the interaction of Cu^{2+} ions at the N7 site of guanines (15,38)). In addition the emergence of the 1542 cm^{-1} band attests that the cytosine N3 atoms are no longer involved in basepairing and are therefore free to interact with the Cu^{2+} ions. The collapse of the duplex structure is also confirmed by the change in the profile of the intense symmetric stretching vibration of the phosphate groups located at 1088 cm^{-1}, very narrow as for a classical B family form duplex for copper/nucleotide ratios below 0.5 and on the contrary broad and weaker for 1 Cu^{2+}/nucleotide, and by the emergence of a strong absorption at 1064 cm^{-1}(Fig. 3).

Triple helix formation at neutral pH stabilized by copper ions

In pyrimidine motif triplexes T·A-T and C^+·G-C bases triplets are expected to form (Fig. 4, *a* and *b*). The latter base triplet requires protonation at the N3 site of the third strand cytosines to allow the establishment of a Hoogsteen-type hydrogen bond with the N7 atom of the guanine in the targeted polypurine strand. Thus acidic pH conditions are required for the formation of such a triple helix. In Fig. 5 are shown the spectra of the equimolecular mixtures of the 14RY duplex and of the 14TC third strand recorded in different conditions, as discussed below. Spectrum 5 *a* obtained at neutral pH is identical to the simulated curve obtained by mathematical addition after normalization of the duplex and third strand spectra (Fig. 5 *curve b*). This rules out any interaction between both entities. When the pH of this mixture is lowered to pH 6, a new spectrum is recorded as displayed in Fig. 5 *c*. This spectrum presents the characteristics of the formation of a classical pyrimidine motif triple helix. The formation of the T·A-T base triplets is detected by the drastic decrease of the thymine ring vibration located in the duplex spectrum at 1637 cm^{-1} and of the adenine band located at 1623 cm^{-1}, assigned to a ND_2 bending vibration coupled to a ring vibration. This latter decrease reflects the binding of the third strand thymine on the ND_2 group, as observed for all triplexes formed by T·A-T or T·A-U base triplets (Fig. 4 *a*) (39–41). The C^+·G-C base triplet formation is characterized by

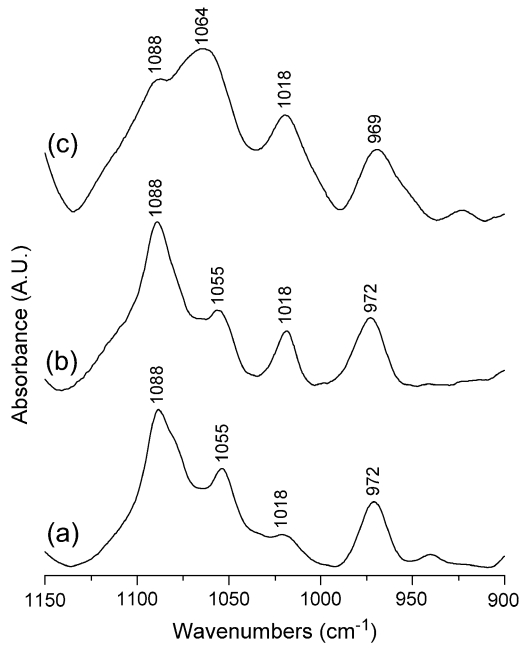

FIGURE 3 FTIR spectra recorded in D_2O solutions at pH 7.2 in the 1150–900 cm^{-1} range of the 14RY duplex in presence of (*a*) 0 Cu^{2+} ion/nucleotide; (*b*) 0.5 Cu^{2+} ion/nucleotide; and (*c*) 1 Cu^{2+} ion/nucleotide.

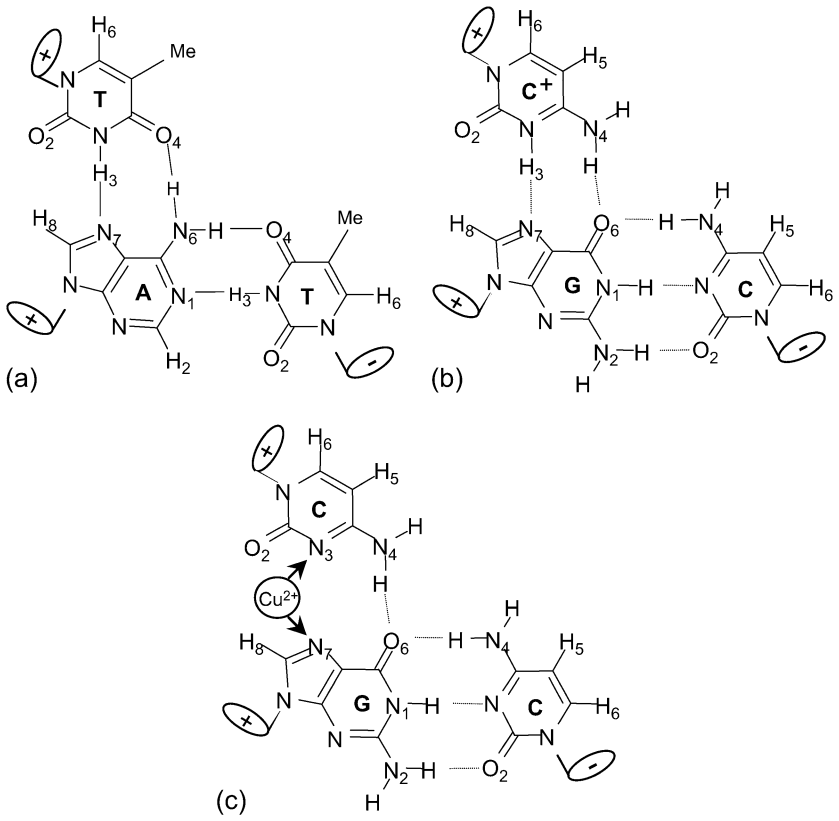

FIGURE 4 Representation of the classical base triplets and of the new proposed C^{Cu}·G-C base triplet involved in pyrimidine triple helix formation. (*a*) T·A-T base triplet. (*b*) C^+·G-C base triplet. The proton of the N3 of the third strand cytosine is forming a hydrogen bond with the N7 of the guanine. (*c*) C^{Cu}·G-C base triplet, Cu^{2+} ions are chelated by the N7 of guanine and the N3 of third strand cytosine.

the emergence of a high wavenumber absorption located above 1700 cm^{-1} (42,43).

The progressive addition of Cu^{2+} ions to the equimolecular mixture 14RY + 14TC enables the stabilization of a triple helix under conditions of neutral pH. We clearly observe in spectrum 5 *d* recorded in presence of 0.5 Cu^{2+} ions/nucleotide all the characteristic features described above: decrease of the relative intensities of the 1623 and 1637 cm^{-1} bands (formation of the T·A-T triplets) and emergence of a band at 1702 cm^{-1}. Cu^{2+} ions are thus able to stabilize the triple helix at neutral pH.

Localization of the copper ions stabilizing the triple helix

The formation of the C·G-C base triplets is thus made possible by the presence of copper ions without protonation of the N3 atom. Different binding sites are possible for Cu^{2+} ions, enabling this binding of the third strand cytosine to the guanine of the target polypurine strand. The proposed binding model (Fig. 4 *c*) is supported by the following evidence.

In the first place, it can be seen that the C6=O6 guanine stretching band located at 1674 cm^{-1} in the duplex spectrum (Fig. 2 *d*) is still present when Cu^{2+} ions are added (Fig. 2 *e*) but is no longer observed in the spectra of the triplexes either at acidic pH (Fig. 5 *c*) or in presence of Cu^{2+} ions (Fig. 5, *d* and *e*). This reflects the formation of the Hoogsteen-type hydrogen bond between the C6=O6 guanine carbonyl and the $N4H_2$ group of the third strand cytosine and does not involve binding of Cu^{2+} ions to the C6=O6 guanine carbonyl.

Second, in the spectrum of the triple helix formed at neutral pH in presence of Cu^{2+} ions (Fig. 5 *d*), an absorption band is detected at 1540 cm^{-1}. We have seen in the previous sections that the emergence of this band reflected the interaction of copper at the N3 atom of cytosines.

The emergence of a band located at 1582 cm^{-1} is also detected in the spectrum of the triple helix formed in presence of Cu^{2+} ions (Fig. 5 *d*), reflecting an interaction at the guanine N7 atom. To confirm the existence of such an interaction, we have studied a triple helix incorporating a targeted purine strand with selectively deuterated guanines at the C8-H group (14D8R). Fig. 6 presents the spectra recorded in H_2O solutions of the 14RY and 14D8RY duplexes (respectively, spectra 6, *a* and *b*). The band located at 1492 cm^{-1} (spectrum 6 *a*) contains a contribution assigned to the N7C8H bending vibration. Hydrogen-deuterium exchange shifts this component to lower wavenumbers: it is now observed at 1462 cm^{-1} (spectrum 6 *b*). Addition of copper ions shifts this band back to 1487 cm^{-1}, reflecting the binding of copper at the N7 guanine site (spectrum 6 *c*).

Now, addition of the third strand to this duplex in presence of copper ions leads to the formation of the triple helix (all characteristic marker bands of triplexes discussed above are observed; see spectrum 5 *e*). In the spectrum of the triplex formed with the selectively deuterated purines recorded in

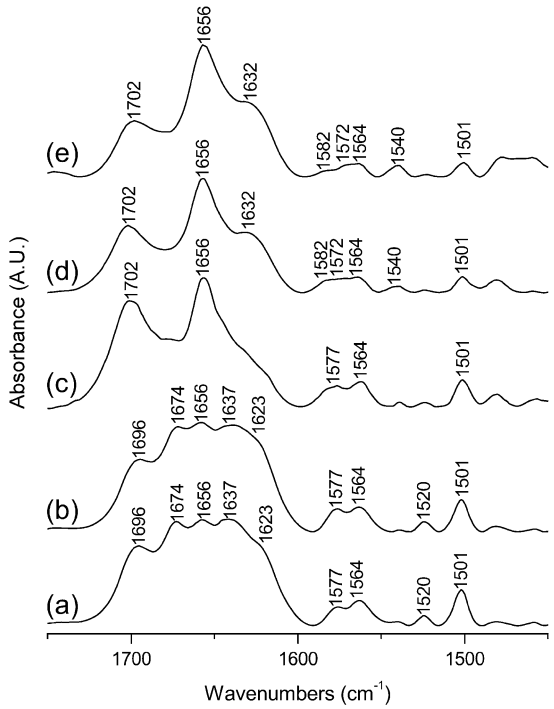

FIGURE 5 FTIR spectra recorded in D_2O solutions in the base in-plane double bond stretching vibration range (1750–1450 cm^{-1}) of (*a*) equimolar mixture of 14RY duplex and 14TC TFO strand at pH 7.2; (*b*) curve obtained by addition of the spectra recorded at pH 7.2 of the 14RY duplex and the 14TC third strand; (*c*) equimolar mixture of 14RY duplex and 14TC TFO strand at pH 6; (*d*) equimolar mixture of 14RY duplex and 14TC TFO strand in presence of 0.5 Cu^{2+} ion/nucleotide at pH 7.2; and (*e*) equimolar mixture of 14D8RY duplex and 14TC TFO strand in presence of 0.5 Cu^{2+} ion/nucleotide at pH 7.2.

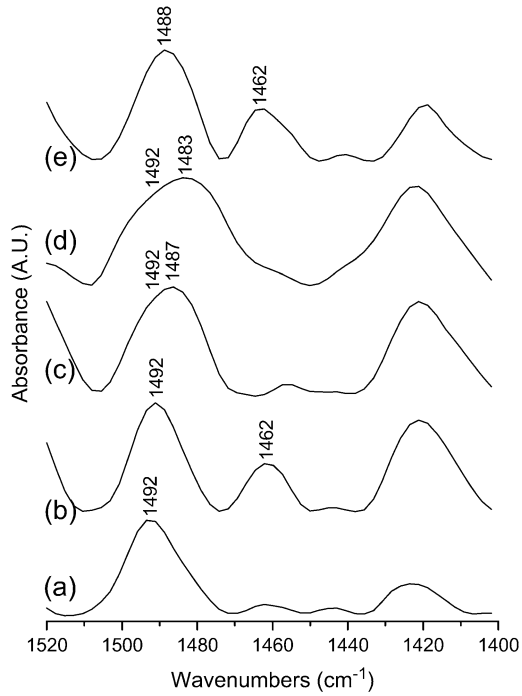

FIGURE 6 FTIR spectra recorded in H_2O solutions in the range 1520–1400 cm^{-1} of (*a*) 14RY duplex at pH 7.2; (*b*) 14D8RY duplex at pH 7.2; (*c*) 14D8RY duplex with 0.5 Cu^{2+} ion/nucleotide at pH 7.2; (*d*) equimolar mixture of 14D8RY duplex and 14TC TFO strand in presence of 0.5 Cu^{2+} ion/nucleotide at pH 7.2; and (*e*) equimolar mixture of 14D8RY duplex and 14TC TFO strand at pH 6.

H_2O solution (Fig. 6 *d*), the guanine N7C8D bending vibration here again is shifted to 1483 cm^{-1}. This shows that the Cu^{2+} ions interact with the N7 site. This shift is due to the interaction with copper ions and not to the formation of the triple helix, as shown by the spectrum of the triple helix formed at acidic pH without Cu^{2+} ions presented in Fig. 6 *e*. In this case the band of the C8 deuterated guanine remains unchanged at 1462 cm^{-1}.

Thus, in the triple helix, the Cu^{2+} ions interact on one hand with the N3 atoms of cytosines and on the other with the N7 atoms of guanines. We propose therefore that they stabilize the formation of the triple helix at neutral pH (Fig. 4 *c*), replacing the protonation of the N3 atom used in classical pyrimidine motif triplexes formed at acidic pH (Fig. 4 *b*).

CONCLUSION

Mechanism of copper-mediated pyrimidic triplex formation: C^{Cu}·G-C

We confirm in this study, by two different techniques (UV and IR spectroscopies), that copper ions can promote the formation of a parallel pyrimidine triplex in vitro under near physiological conditions. We thus demonstrate that the classical Hoogsteen hydrogen bond between the N3 atom of the protonated cytosine in the third strand and the N7 atom of the guanine in the duplex is replaced by a copper ion as shown in Fig. 4 *c*. Such a C^{Cu}·G-C triplex exhibits characteristics different from those of a classical pyrimidine triplex. Although the T_m of the copper-mediated triplex is lower than that of the acidic triplex, its melting transition appears reversible upon association and dissociation. Competing experiments performed between the two ways of forming the *Drosophila* satellite triple helix (i.e., under acidic conditions or when 0.5 Cu^{2+} ion/nucleotide is added at neutral pH; data not presented) show that formation of the classical C^+·G-C base triplets is always preferred over that of C^{Cu}·G-C bases triplets. Thus, the two mechanisms of triplex formation, copper-mediated or N3 protonation-mediated, appear mutually exclusive. Such data are consistent with the possibility of triple helix formation in vivo in a broader range of conditions, including local acidic pH and local neutral pH in presence of Cu^{2+} ions.

Biological relevance of triplexes in heterochromatin

A question that arises here is: Can triple helices, or H-DNA, be formed in vivo in centromeric regions? Some studies have

shown that TFOs can be hybridized in situ to nondenatured metaphase spreads and interphase nuclei (44) and that triplex-forming DNAs in the human interphase nucleus can be visualized with DNA probes and anti-triplex antibodies (45). Our results show that, in principle, the *Drosophila* AG-rich satellite is able to form a triple helix. Yet, a major restriction (the necessity of an acidic pH) could prevent the formation of this pyrimidine triple strand structure in vivo. We demonstrate in this study that pH dependence can be overcome by relatively low Cu^{2+} concentrations.

It is conceivable that some intracellular mechanisms can locally increase divalent metal ions concentrations to levels comparable with our experimental conditions. For example, it is known that metal ions are naturally present in in vivo DNA (18) and concentrated in centromeric reiterated sequences (2,7). Thus, high local concentrations of divalent cations can be achieved via their natural binding to such sequences. Another mechanism by which the triplex-modulatory effects that we have observed with naked transition metal cations could be accomplished naturally in vivo is the interaction with a metal cation coordinated to a specialized peptide domain (46) or by a conjugate such as iminodiacetic acid (47) or glutamic acid (48).

Our data have been obtained using a twice-repeated AAGAGAG target sequence of the *D. melanogaster* satellite DNA. In vivo the sequence is found repeated thousands of times. We have previously shown (19) that an increase in the number of repeats drastically increases the triplex stability. Thus we can reasonably propose that the formation of a stable copper-induced triplex in vivo may be compatible with the environmental conditions naturally encountered by *D. melanogaster* (49).

Thus the data presented herein support the concept that triplex-favorable local conditions of the micronuclear environment and therefore triple-stranded DNA can exist in vivo. The study of the effect of other metal ions on the stabilization of triple helices in *D. melanogaster* satellite repeats is now under progress.

We are grateful to Dr. C. Herve du Penhoat for proofreading the manuscript. J. Lacoste would like to thank EA and EG.

REFERENCES

1. Sorokin, V. A., V. A. Valeev, G. O. Gladchenko, I. V. Sysa, Y. P. Blagoi, and I. V. Volchok. 1996. Interaction of bivalent copper, nickel, manganese ions with native DNA and its monomers. *J. Inorg. Biochem.* 63:79–98.
2. Guillé, E., J. Grisvard, and I. Sissoëff. 1979. Implications of reiterative DNA-metal ion complexes in the induction and development of neoplastic cells. Biol. Trace Elem. Res. 1:299–311.
3. Coogan, T. P., D. M. Latta, R. J. Imbra, and M. Costa. 1989. Effect of nickel(II) on DNA-protein interactions. *Biol. Trace Elem. Res.* 21:13–21.
4. Bernues, J., R. Beltran, J. M. Casasnovas, and F. Azorin. 1990. DNA-sequence and metal-ion specificity of the formation of *H-DNA. *Nucleic Acids Res.* 18:4067–4073.
5. Frank-Kamenetskii, M. D., and S. M. Mirkin. 1995. Triplex DNA structures. *Annu. Rev. Biochem.* 64:65–95.
6. Guillé, E., J. Grisvard, and I. Sissoëff. 1981. Structure and function of metallo-DNA in the living cell. *In* Systemic Aspects of Biocompatibility. D. Williams, editor. CRC Press, Boca Raton, FL. 39–141.
7. Sissoeff, I., J. Grisvard, and E. Guillé. 1976. Studies on metal ions-DNA interactions: specific behaviour of reiterative DNA sequences. *Prog. Biophys. Mol. Biol.* 31:165–199.
8. Heitz, E. 1928. Das Heterochromatin der Moose. *Jahrb. Wiss. Bot.* 69:762–818.
9. Hoskins, R. A., C. D. Smith, J. W. Carlson, A. B. Carvalho, A. Halpern, J. S. Kaminker, C. Kennedy, C. J. Mungall, B. A. Sullivan, G. G. Sutton, J. C. Yasuhara, B. T. Wakimoto, E. W. Myers, S. E. Celniker, G. M. Rubin, and G. H. Karpen. 2002. Heterochromatic sequences in a *Drosophila* whole-genome shotgun assembly. *Genome Biol.* 3:research0085.0081–0085.0016.
10. Verma, R. S. 1988. Heterochromatin. Molecular and Structural Aspects. R. S. Verma, editor. Cambridge University Press, Cambridge.
11. Sun, X., J. Wahlstrom, and G. Karpen. 1997. Molecular structure of a functional Drosophila centromere. *Cell.* 91:1007–1019.
12. Sun, X., H. D. Le, J. M. Wahlstrom, and G. H. Karpen. 2003. Sequence analysis of a functional Drosophila centromere. *Genome Res.* 13:182–194.
13. Horvath, J. E., S. Schwartz, and E. E. Eichler. 2000. The mosaic structure of human pericentromeric DNA: a strategy for characterizing complex regions of the human genome. *Genome Res.* 10:839–852.
14. Tajmir-Riahi, H. A., M. Naoui, and R. Ahmad. 1993. The effects of Cu2+ and Pb2+ on the solution structure of calf thymus DNA: DNA condensation and denaturation studied by Fourier transform IR difference spectroscopy. *Biopolymers.* 33:1819–1827.
15. Andrushchenko, V., J. H. van de Sande, and H. Wieser. 2003. Vibrational circular dichroism and IR absorption of DNA complexes with Cu2+ ions. *Biopolymers.* 72:374–390.
16. Zimmer, C., G. Luck, H. Fritzsche, and H. Triebel. 1971. DNA-copper (II) complex and the DNA conformation. *Biopolymers.* 10:441–463.
17. Malkov, V. A., O. N. Voloshin, V. N. Soyfer, and M. D. Frank-Kamenetskii. 1993. Cation and sequence effects on stability of intermolecular pyrimidine-purine-purine triplex. *Nucleic Acids Res.* 21:585–591.
18. Sagripanti, J. L., P. L. Goering, and A. Lamanna. 1991. Interaction of copper with DNA and antagonism by other metals. *Toxicol. Appl. Pharmacol.* 110:477–485.
19. Horn, V., L. Lacroix, T. Gautier, M. Takasugi, J. L. Mergny, and J. Lacoste. 2004. Triple helix formation with Drosophila satellite repeats. Unexpected stabilization by copper ions. *Biochemistry.* 43:11196–11205.
20. Mills, M., P. B. Arimondo, L. Lacroix, T. Garestier, C. Hélène, H. Klump, and J. L. Mergny. 1999. Energetics of strand-displacement reactions in triple helices: a spectroscopic study. *J. Mol. Biol.* 291: 1035–1054.
21. Le Doan, T., L. Perrouault, D. Praseuth, N. Habhoub, J. L. Decout, N. T. Thuong, J. Lhomme, and C. Helene. 1987. Sequence-specific recognition, photocrosslinking and cleavage of the DNA double helix by an oligo-[alpha]-thymidylate covalently linked to an azidoproflavine derivative. *Nucleic Acids Res.* 15:7749–7760.
22. Moser, H. E., and P. B. Dervan. 1987. Sequence-specific cleavage of double helical DNA by triple helix formation. *Science.* 238:645–650.
23. Beal, P. A., and P. B. Dervan. 1991. Second structural motif for recognition of DNA by oligonucleotide-directed triple-helix formation. *Science.* 251:1360–1363.
24. Mills, M., L. Lacroix, P. B. Arimondo, J. L. Leroy, J. C. Francois, H. Klump, and J. L. Mergny. 2002. Unusual DNA conformations: implications for telomeres. *Curr. Med. Chem. Anti-Canc. Agents.* 2:627–644.
25. Chan, P. P., and P. M. Glazer. 1997. Triplex DNA: fundamentals, advances, and potential applications for gene therapy. *J. Mol. Med.* 75: 267–282.
26. Sun, J. S., T. De Bizemont, G. Duval-Valentin, T. Montenay-Garestier, and C. Helene. 1991. Extension of the range of recognition sequences for triple helix formation by oligonucleotides containing guanines and thymines. *C. R. Acad. Sci. III.* 313:585–590.

27. Adam, S., P. Bourtayre, J. Liquier, and E. Taillandier. 1986. Interaction of transition metal ions with Z form poly d(A-C).poly d(G-T) and poly d(A-T) studied by I.R. spectroscopy. *Nucleic Acids Res.* 14:3501–3513.

28. Adam, S., P. Bourtayre, J. Liquier, J. A. Taboury, and E. Taillandier. 1987. Poly[d(A-T)-Cs+] conformations studied by IR spectroscopy. *Biopolymers.* 26:251–260.

29. Taillandier, E., and J. Liquier. 1992. Infrared spectroscopy of DNA. *Methods Enzymol.* 211:307–335.

30. Tsuboi, M., K. Shuto, S. Takemura, and S. Nishimura. 1969. Infrared spectra of a few transfer ribonucleic acids. *Bull. Chem. Soc. Jpn.* 42: 102–107.

31. Taboury, J., J. Liquier, and E. Taillandier. 1985. Characterization of DNA structures by infrared spectroscopy: double helical forms of poly (dG-dC), poly (dD8G-dC) and poly (dG-dm5C). *Can. J. Chem.* 63: 1904–1909.

32. Cantor, C. R., M. M. Warshaw, and H. Shapiro. 1970. Oligonucleotide interactions. 3. Circular dichroism studies of the conformation of deoxyoligonucleotides. *Biopolymers.* 9:1059–1077.

33. Rougée, M., B. Faucon, J. L. Mergny, F. Barcelo, C. Giovannangeli, T. Garestier, and C. Hélène. 1992. Kinetics and thermodynamics of triple-helix formation: effects of ionic strength and mismatches. *Biochemistry.* 31:9269–9278.

34. Taillandier, E., and J. Liquier. 2002. Vibrational spectroscopy of nucleic acids. *In* Handbook of Vibrational Spectroscopy. J. M. Chalmers and P. R. Griffith, editors. John Wiley. 3465–3480.

35. Rush III, T., H. Yong, and W. L. Peticolas. 1997. Structure and stability of cytosine deoxyoligonucleotides multiplexes. *Biopolymers.* 41:121–130.

36. Eichhorn, G. L., P. Clark, and E. D. Becker. 1966. Interactions of metal ions with polynucleotides and related compounds. VII. The binding of copper(II) to nucleosides, nucleotides, and deoxyribonucleic acids. *Biochemistry.* 5:245–253.

37. Fritzsche, H., and C. Zimmer. 1968. Infrared studies of deoxyribonucleic acids, their constituents and analogues. 4. The binding sites of copper(II) in DNA. *Eur. J. Biochem.* 5:42–44.

38. Hackl, E. V., S. V. Kornilova, and Y. P. Blagoi. 2005. DNA structural transitions induced by divalent metal ions in aqueous solutions. *Int. J. Biol. Macromol.* 35:175–191.

39. Liquier, J., P. Coffinier, M. Firon, and E. Taillandier. 1991. Triple helical polynucleotidic structures: sugar conformations determined by FTIR spectroscopy. *J. Biomol. Struct. Dyn.* 9:437–445.

40. Dagneaux, C., J. Liquier, and E. Taillandier. 1995. FTIR study of a nonclassical dT10*dA10-dT10 intramolecular triple helix. *Biochemistry.* 34:14815–14818.

41. Guzman, M. R., J. Liquier, and E. Taillandier. 2005. Hydration and conformational transitions in DNA, RNA, and mixed DNA-RNA triplexes studied by gravimetry and FTIR spectroscopy. *J. Biomol. Struct. Dyn.* 23:331–339.

42. Akhebat, A., C. Dagneaux, J. Liquier, and E. Taillandier. 1992. Triple helical polynucleotidic structures: an FTIR study of the C+ .G. Ctriplet. *J. Biomol. Struct. Dyn.* 10:577–588.

43. Liquier, J., and E. Taillandier. 1996. Infrared spectroscopy of nucleic acids. *In* Infrared Spectroscopy of Biomolecules. H. H. Mantsch and D. J. Chapman, editors. Wiley-Liss.

44. Johnson 3rd, M. D., and J. R. Fresco. 1999. Third-strand in situ hybridization (TISH) to non-denatured metaphase spreads and interphase nuclei. *Chromosoma.* 108:181–189.

45. Ohno, M., T. Fukagawa, J. S. Lee, and T. Ikemura. 2002. Triplex-forming DNAs in the human interphase nucleus visualized in situ by polypurine/polypyrimidine DNA probes and antitriplex antibodies. *Chromosoma.* 111:201–213.

46. Eichhorn, G. L., P. P. Chuknyisky, J. J. Butzow, R. B. Beal, C. Garland, C. P. Janzen, P. Clark, and E. Tarien. 1994. A structural model for fidelity in transcription. *Proc. Natl. Acad. Sci. USA.* 91: 7613–7617.

47. Sueda, S., T. Ihara, and M. Takaki. 1997. Metallo-regulation of DNA triple helix formation through cooperative dimerization of two oligonucleotides. Chem. Letter. 26:1085–1088.

48. Ihara, T., Y. Takeda, and A. Jyo. 2001. Metal ion-directed cooperative triple helix formation of glutamic acid-oligonucleotide conjugate. *J. Am. Chem. Soc.* 123:1772–1773.

49. James, A. C., R. B. Azevedo, and L. Partridge. 1997. Genetic and environmental responses to temperature of Drosophila melanogaster from a latitudinal cline. *Genetics.* 146:881–890.